



Isotope fractionation of alkaline and alkaline-earth elements (Li, K, Rb, Mg, Ca, Sr, Ba) during diffusion in aqueous solutions

Weiqliang Li^{*}, Zhihan Ji, Xianglong Luo, Yuqi Li

State Key Laboratory for Mineral Deposits Research, School of Earth Sciences and Engineering, Nanjing University, Nanjing, Jiangsu 210093, PR China

ARTICLE INFO

Associate editor: Jeffrey G Catalano

Keywords:

Diffusion
Isotope fractionation
Alkaline elements
Alkaline-earth elements
Aqueous solution

ABSTRACT

In this study, we used an improved “diffusion cell” method to precisely determine the diffusion-driven kinetic isotope fractionation factors of the Li, K, Rb, Mg, Ca, Sr, and Ba cations in aqueous solutions under room temperature. The obtained isotope fractionation factors ($\pm 2\sigma$ errors) are, $\alpha_{7/6\text{Li}} = 0.996139 \pm 0.000140$, $\alpha_{41/39\text{K}} = 0.998572 \pm 0.000072$, $\alpha_{87/85\text{Rb}} = 0.999333 \pm 0.000020$, $\alpha_{26/24\text{Mg}} = 0.999877 \pm 0.000010$, $\alpha_{44/42\text{Ca}} = 0.999704 \pm 0.000010$, $\alpha_{88/86\text{Sr}} = 0.999781 \pm 0.000014$, $\alpha_{138/135\text{Ba}} = 0.999716 \pm 0.000018$. The results show that the charge of the cation and the ion-water bond length for the aquo ions are the two predominant factors affecting the mass dependence of isotope fractionation (β factor) during cation diffusion in aqueous solutions. Cations with higher charge numbers and shorter ion-water bond lengths exhibit less kinetic isotope fractionation during diffusion. Therefore, the isotope separation effect during diffusion (or β factor) in fluids is fundamentally controlled by the intensity of ion-water interaction. Weaker ion-water interaction (e.g., lower charge number, longer ion-water bond length) leads to less prominent hydrodynamic behavior for diffusing ions at the molecular level, thus more significant isotope fractionation in bulk solutions, and vice versa. Ions of larger radius would show stronger mass dependence of isotope fractionation (β factor), which can cancel the effect of decreasing relative isotope mass difference for heavier elements, thus kinetic isotope fractionation during diffusion in aqueous solutions remains prominent even for heavy elements such as Rb, Sr, and Ba. The diffusion-driven kinetic isotope fractionation factors measured in this study could provide a useful basis for interpreting specific natural isotopic variability of alkaline and alkaline-earth elements in supergene environments where chemical diffusion takes place.

1. Introduction

Diffusion is a fundamental kinetic process that can occur in response to concentration gradients in gases, liquids, or solids. Because the diffusion rates of molecular-level particles (i.e., atom, ion, molecule) could be dependent on their mass, kinetic isotope fractionation arises during diffusion driven by concentration gradients of elements that have multiple stable isotopes (Richter et al., 2009). Aqueous solutions in Earth's surficial environment are the hot spot of chemical reactions and disequilibrium. For example, pore water near the sediment–water interface hosts various concentration gradients of dissolved components, where chemical diffusion and diffusion-driven isotope fractionation can take place (Cao et al., 2023; Schulz, 2006). Quantification of kinetic isotope fractionation factor ($\alpha = D^*/D$, the ratio of diffusion coefficients between the heavy and light isotopes) associated with diffusion in aqueous solutions is a prerequisite for proper interpretation

of the isotopic variability observed in natural samples from such environments of chemical disequilibrium. Isotope fractionation of different gas molecules during diffusion in aqueous solutions had been studied by experiments (e.g., Jähne et al., 1987; O'Leary, 2002; Tyroller et al., 2018; Tyroller et al., 2014) and molecular dynamics simulations (Bourg and Sposito, 2008; Pinto de Magalhães et al., 2017), and the computational results agree well with experimental results, due to the effective approximation of intermolecular interactions by elastic collisions of simple particles. Diffusion of ions in aqueous solutions, however, is more complex than diffusion of gas molecules, and it involves intermolecular processes beyond purely translational motion and elastic collisions of simple particles (Wanner and Hunkeler, 2019). Despite the challenges, significant progresses have been made in understanding the general behavior of isotope fractionation during diffusion of ions in aqueous solution in recent years (Bourg et al., 2010; Wanner and Hunkeler, 2019; Watkins et al., 2017).

^{*} Corresponding author.

E-mail address: liweiqiang@nju.edu.cn (W. Li).

Alkaline and alkaline-earth elements are two groups of highly soluble elements, and seven of them (Li, K, Rb, Mg, Ca, Sr, Ba) have multiple stable isotopes. Diffusion-driven kinetic isotope fractionation of five of these elements (i.e., Li, K, Mg, Ca, Ba) in aqueous solutions had been investigated based on experiments (e.g., Bourq et al., 2010; Richter et al., 2006; van Zuilen et al., 2016) and computer simulations (e.g., Bourq et al., 2010; Bourq and Sposito, 2007). The different methods used in generating the isotope fractionation factors may introduce issues of inconsistency, which limits in-depth discussions into the systematics of diffusion-driven isotope fractionation for alkaline and alkaline-earth cations. Further, the diffusion-driven isotope fractionation factors for Rb and Sr in aqueous solutions remain unknown. In this study, we developed a modified “diffusion cell” method with improved precision and efficiency, for determination of the kinetic isotope fractionation factors associated with diffusion of solute in aqueous solutions. Using this method, we obtained the kinetic isotope fractionation factors of Li, K, Rb, Mg, Ca, Sr, and Ba during diffusion in aqueous solutions. The obtained results can serve as a basis for interpreting natural isotopic variability caused by diffusion and may further shed insights into the molecular-level dynamics of cation diffusion in aqueous solutions.

2. Experimental concept

Different experimental approaches have been adopted for the determination of kinetic isotope fractionation factors associated with diffusion in aqueous solutions, including 1) direct sampling of the aqueous solution/gel in different segments of a diffusion profile (Eggenkamp and Coleman, 2009; Rodushkin et al., 2004), 2) to conduct diffusion experiment across the membrane of a diffusion cell (called diaphragm-cell in some literature) and analyze the solute at both sides of the membrane after a certain period (O’Leary, 2002; Stokes, 1950), and 3) analysis of residual solute within a diffusion cell after variable degrees of diffusional loss of solute (Christensen et al., 2019; Richter et al., 2006). The last approach is also called Graham’s type diffusion experiments.

In this study, we used a modified Graham’s type diffusion approach to investigate isotope fractionation of metal cations during diffusion in aqueous solution. The experimental setup is illustrated in Fig. 1A. This experimental setup is similar to the “diffusion cell” method that has been described by Wanner and Hunkeler (2015). For each experiment, a stock solution was added into a diffusion cell that has a membrane at the bottom. The diffusion cell was placed in a flow-through container, where a constant stream of de-ionized water was flushing through the bottom of the diffusion cell. During this process, the solute in the cell diffused

across the membrane into the deionized water and was transported away by a peri-pump. An automatic fraction collector was used to collect the flushing solute into a series of centrifuge tubes consecutively, with a constant time step.

Based on the elemental concentration and volume data for the collected solutions in tubes and the cell, the fraction of cation remaining in the diffusion cell (f) at each tube-switching time point can be calculated following the equation:

$$f = \frac{\sum_{i+1}^n (C_{\text{tube}}^{i+1} \times V_{\text{tube}}) + C_{\text{cell}}^n \times V_{\text{cell}}}{C_{\text{cell}}^0 \times V_{\text{cell}}} = \frac{\sum_{i+1}^n (C_{\text{tube}}^{i+1} \times V_{\text{tube}}) + C_{\text{cell}}^n \times V_{\text{cell}}}{\sum_{i+1}^n (C_{\text{tube}}^i \times V_{\text{tube}}) + C_{\text{cell}}^n \times V_{\text{cell}}} \quad (1)$$

where V and C are the volume and the cation concentration of aqueous solution in the tube or cell, respectively. Superscript i denotes the i^{th} tube, and superscripts 0 and n denote the number of starting and ending cell, respectively.

Diffusing of solute out of the diffusion cell into pure water follows a Rayleigh behavior. Given that light isotopes diffuse more rapidly than heavy isotopes, the solute remaining in the diffusion cell will become isotopically heavier with the progression of diffusion. It has been well established that, under ideal situations, the isotope composition of the solute in the cell (δ_{cell}) covaries with $-\ln f$, defining a linear trend on a plot of δ versus $-\ln f$ (Fig. 1B, cell trend), and the slope of the trend is a simple function of diffusion-driven isotope fractionation factor α (i.e., slope = $-1000\ln\alpha$) (Richter et al., 2006; Wanner and Hunkeler, 2015). This relation can be expressed as

$$\delta_{\text{cell}}^i = \ln f \cdot 1000\ln\alpha + \delta_{\text{cell}}^0 \quad (2)$$

It can be further proven that, for the diffusion cell experiments in this study, the isotope composition of the flushing solute collected in the tubes (δ_{tube}) plot along a secondary linear trend parallel to the cell trend on the same δ versus $-\ln f$ plot (Fig. 1B, tube trend), such as

$$\delta_{\text{tube}}^i = \ln f \cdot 1000\ln\alpha + (\delta_{\text{cell}}^0 + k) \quad (3)$$

where k is a constant related to the membrane of the diffusion cell and the diffusing characteristics of the solute. The proof for the fact that the slope of the data trend of δ versus $-\ln f$ for the tube also equals $-1000\ln\alpha$ is provided in Supplementary material S1.

In previous studies that used the diffusion cell method to quantify the fractionation of isotopes during diffusion in aqueous solutions, f and δ values were measured from solutions remaining in the diffusion cell (Bourq et al., 2010; Richter et al., 2006; Wanner and Hunkeler, 2015). In

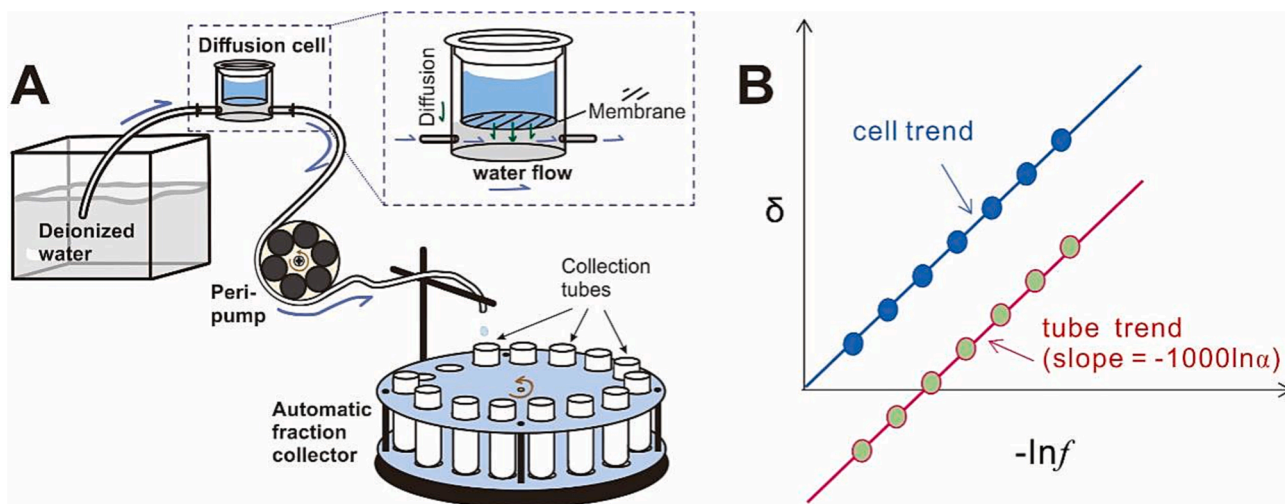


Fig. 1. A. Sketch of the experimental set-up for the diffusion cell method. B. Illustration of the key concept of obtaining diffusion driven isotope fractionation factor α from the diffusion cell experiment, note the linear correlation between the isotope composition of solutes in the diffusion cell and the tubes (δ_{cell} and δ_{tube}) and $-\ln f$.

such an approach, each diffusion experiment only produces one data point, and multiple diffusion experiments are needed to generate a data trend for the calculation of the diffusional isotope fractionation factor α (Fig. 1B, the cell trend). In this study, the f and δ values were obtained from multiple fractions of the solute diffused out of the diffusion cell (Fig. 1B, the tube trend), thus only one diffusion experiment is needed for the calculation of slope in the δ versus $-\ln f$ plot (Fig. 1B, the tube trend), and the efficiency is significantly improved. Note that in our method the f values are associated with greater error compared to the classic diffusion cell method (e.g., in Richter et al., 2006), as the f values are calculated based on summation of measured solute contents from multiple tubes, which suffers from error propagation of multiple measurements. Nonetheless, because the new method enables high-density sampling of the flushing solutions, more data points can be generated in the δ versus $-\ln f$ plot, which can yield better precision for slope calculation by linear regression.

3. Experiments and analyses

3.1. The diffusion cell experiments

Reagents grade salts of LiCl, KCl, RbCl, Mg(NO₃)₂, CaCl₂, SrCl₂, and BaCl₂ were individually dissolved in deionized water to prepare stock solutions with cation concentrations around 10,000 ppm. For each experiment, a 2 ml stock solution of the solute of interest (e.g., 10000 ppm Li as LiCl) was added into a diffusion cell. The diffusion cell is a part of the Slide-A-Lyer® dialysis kit from Thermo Scientific for life sciences, it has a ~30 μm thick, one inch (2.5 cm) round dialysis membrane with molecular weight cut off (MWCO) of 3500 Dalton at the bottom. Before the diffusion experiment, the membrane was soaked in 2 % HNO₃ overnight followed by rinsing in deionized water for cleaning.

The diffusion cell was placed on a rocking stage that rocked between +10° and -10° at 40 Hz, to homogenize the solutions within the cell and minimize the boundary layers at both sides of the membrane. The diffusion cell was placed in a custom-made flow-through container in an air-conditioned room at 25 °C. For the diffusion experiment, de-ionized water was flushed through the bottom of the diffusion cell by a peristaltic pump at a rate of 6.5 ml/hour, and the flushing solution was collected in 10 ml plastic tubes for every one-hour time bracket with an automatic fraction collector.

3.2. Elemental analysis

Elemental concentrations of the solutions (except for those of K) from the diffusion experiments were measured on an inductively-coupled plasma optical emission spectrometer (ICP-OES, Skyray type ICP-3000) at State Key Laboratory of Mineral Deposits Research, Nanjing University. For the concentration of K in solutions from the KCl diffusion experiments, the measurement was performed using a flame photometer. A series of gravimetrically prepared single or multi-element standard solutions (0, 0.05 ppm, 0.1 ppm, 0.5 ppm, 1 ppm, 5 ppm, 10 ppm) were used as the calibration standards. The sample solutions were diluted to 1–5 ppm for concentration measurements. The variable concentration standard solutions were measured before and after each analytical session, and a 1 ppm standard solution was measured between every 10 samples to monitor and correct for instrument drift. The analytical uncertainty of elemental concentration measurement was better than ±5 % (RSD).

3.3. Isotope analysis

Isotope ratios of the seven alkaline and alkaline-earth elements were measured on a Nu 1700 Sapphire MC-ICP-MS at Nanjing University. The instrumental parameters for the measurement of the different isotope systems are summarized in Table S2 of Supplementary Materials. For all analyses in this study, the instrument was running with the conventional

“high-energy” path (i.e., collision cell path disabled), with a standard 1300w forward power and 6000v acceleration voltage. Each isotope analysis consisted of 40 ratios of 4-second integration, and a 3-minute wash in 2 % HNO₃ was applied between each isotope analysis to minimize cross-contamination. Sample-standard bracketing was used to correct for mass bias and instrument drift during analysis, and the initial solutions of the diffusion experiments were used as the bracketing standards. The concentrations of samples and standard solutions were matched within ±10 %. Typically, each sample was measured 3 or 4 times, and the average and 2 standard deviations (2SD) of the multiple analytical results are reported. The measured isotope data are expressed in δ notation

$$\delta = (R_{\text{sample}}/R_{\text{standard}} - 1) \times 1000 \quad (4)$$

where R is the ratio of heavy to light isotopes, and the original stock solution for each diffusion experiment was used as the standard.

For isotope analysis of K and Ca, the instrument was running on dry plasma and high mass resolution mode, with detailed mass spectrometer settings reported in An et al. (2022). The analyte solutions were introduced into the ICP through an Aridus III desolvator. High mass resolution (mass resolving power > 16000) was used for resolving the polyatomic interferences from the isotopes of interest (i.e., ArH⁺ on ⁴¹K⁺ during K isotope analysis; CNO⁺ on ⁴²Ca⁺ during Ca isotope analysis). The typical internal precision of ⁴¹K/³⁹K ratio measurement was better than ±0.04 ‰ (2SE), and long-term external reproducibility was better than ±0.07 ‰ (2SD). For Ca isotopes, the typical internal precision of ⁴⁴Ca/⁴²Ca ratio measurement was better than 0.05 ‰ (2SE), and short-term (in-run) external precision was on the level of ±0.10 ‰ (2SD).

For isotope analysis of Li, Rb, Mg, Sr, and Ba, the instrument was running on wet plasma and low mass resolution mode, with a typical mass spectrometer setting as described in Liu and Li (2023). For these analyses, 500 ppb of the analyte solutions were introduced into the ICP via a cyclonic spray chamber. The typical internal precision (2SE) of isotope ratio analyses was better than ±0.20 ‰ for ⁷Li/⁶Li, ±0.04 ‰ for ²⁶Mg/²⁴Mg, ±0.04 ‰ for ⁸⁷Rb/⁸⁵Rb, ±0.05 ‰ for ⁸⁸Sr/⁸⁶Sr, and ±0.04 ‰ for ¹³⁸Ba/¹³⁵Ba; the short-term (in-run) external precision (2SD) was on the level of ±0.70 ‰ for ⁷Li/⁶Li, ±0.10 ‰ for ⁸⁸Sr/⁸⁶Sr, ±0.08 ‰ for ⁸⁷Rb/⁸⁵Rb and ¹³⁸Ba/¹³⁵Ba; the long-term external reproducibility of ²⁶Mg/²⁴Mg measurements was on the level of ±0.10 ‰.

4. Results

During each diffusion experiment, the concentration of cation in the tube decreased exponentially with time (Fig. 2; Tables S3-1 to S3-7), which followed a Rayleigh behavior. The fraction of cation remaining in the diffusion cell (f), calculated using Eq. (1), also decreased exponentially with time by and large (Fig. 2; Tables S3-1 to S3-7). In the plot of f versus time (Fig. 2A), the slope of the data trend of Li was less steep than those of Rb and K, implying a slightly slower diffusion of Li among the alkaline elements. Similarly, Mg shows a less steep data trend than Ca in a plot of f versus time (Fig. 2B), indicating a slightly lower diffusivity of Mg compared to Ca.

The isotope compositions (δ values) of the cations in the tubes increased systematically with time in each of the diffusion experiments (Fig. 3; Tables S3-1 to S3-7), but the change in δ values varied remarkably between different isotope systems. As illustrated in Fig. 3, $\delta^{7/6}\text{Li}$ values of solutes in the tubes increased by ~12 ‰, and the $\delta^{41/39}\text{K}$ and $\delta^{87/85}\text{Rb}$ values of the solute in the tubes increased by ~5 ‰ and ~1.9 ‰ during the diffusion experiments, respectively. For alkaline-earth elements, the increases in δ values of the solute in tubes were ~0.7 ‰ for $\delta^{26/24}\text{Mg}$, ~1.5 ‰ for $\delta^{44/42}\text{Ca}$, ~0.6 ‰ for $\delta^{88/86}\text{Sr}$, and ~1.0 ‰ for $\delta^{138/135}\text{Ba}$ during the diffusion experiments.

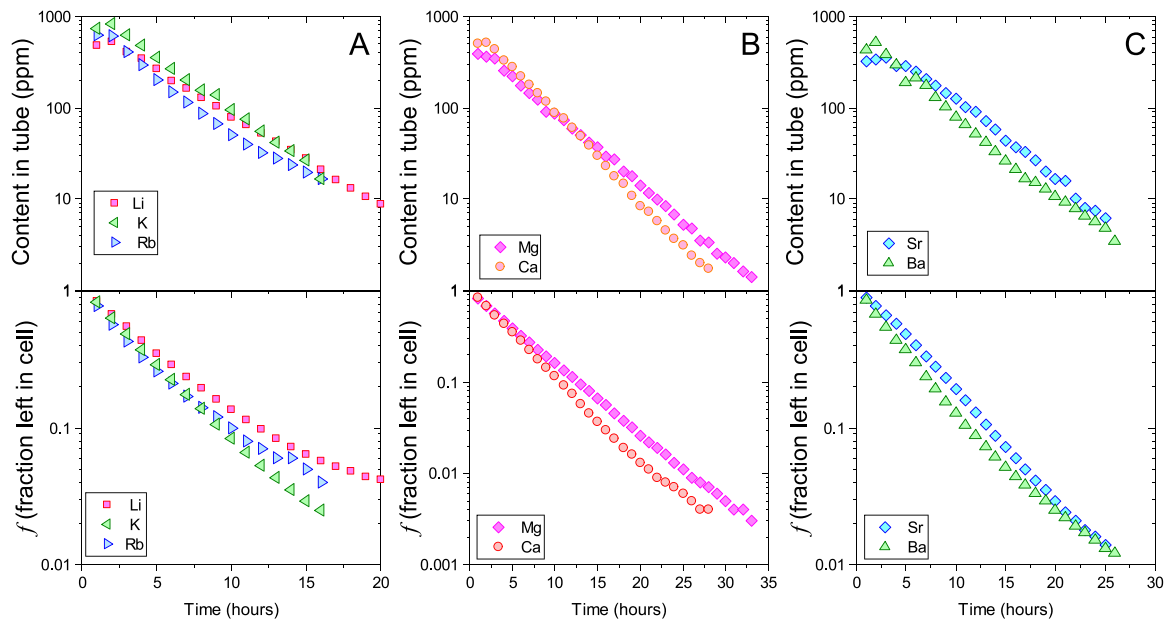


Fig. 2. Change of the content of cations in the tube, and the corresponding f (the fraction of the cation left in the diffusion cell) as a function of time in the diffusion experiments for Li, K, Rb (plot A), Mg, Ca (plot B), and Sr and Ba (plot C).

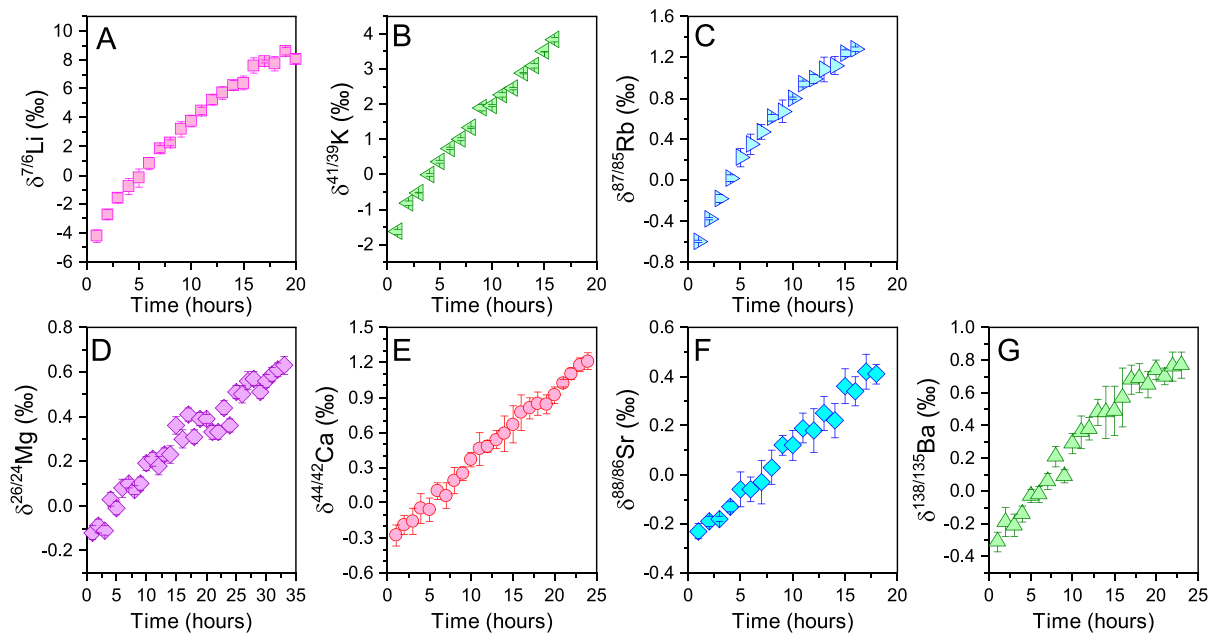


Fig. 3. Change of the isotope composition of cations (in δ relative to starting solution) in the tube with time in the diffusion experiments for Li (A), K (B), Rb (C), Mg (D), Ca (E), Sr (F), and Ba (G).

5. Discussions

5.1. Isotope fractionation during the diffusion experiments for the seven elements

At the beginning of each diffusion experiment, the isotope composition of the solute in the collection tube was lighter than the stock solution (i.e., $\delta < 0$; Fig. 3), reflecting preferential diffusion of light isotopes into the deionized water through the membrane. As a result of this process, the solute remaining in the cell became isotopically heavier. Subsequently, the solute collected in the tubes became increasingly enriched in heavy isotopes, and eventually became isotopically heavier than the initial stock solution ($\delta > 0$). The transition from $\delta < 0$ to $\delta > 0$

for the solutes in the tubes is expected to occur at $-\ln f$ of 1. This is because according to Eq. (2), the δ value of the solute in the diffusion cell would be elevated by a factor of $-1000 \ln \alpha$ when $-\ln f$ equals 1, and at this point, the solute diffuses out of the membrane would have a δ of zero due to the offset by diffusion isotope fractionation effect α . Such transition of $\delta < 0$ to $\delta > 0$ for solutes in the tube occurred at $-\ln f$ of 1 for all experiments (Fig. 4), exactly matching the theoretical prediction.

Furthermore, all experiments need to obey the conservation of isotope mass balance, according to the following equation:

$$\delta_{\text{cell}}^0 = \frac{\sum_i^n (C_{\text{tube}}^i \times V_{\text{tube}}) \times \delta_{\text{tube}}^i + C_{\text{cell}}^n \times V_{\text{cell}} \times \delta_{\text{cell}}^n}{\sum_i^n (C_{\text{tube}}^i \times V_{\text{tube}}) + C_{\text{cell}}^n \times V_{\text{cell}}} = 0(\%) \quad (5)$$

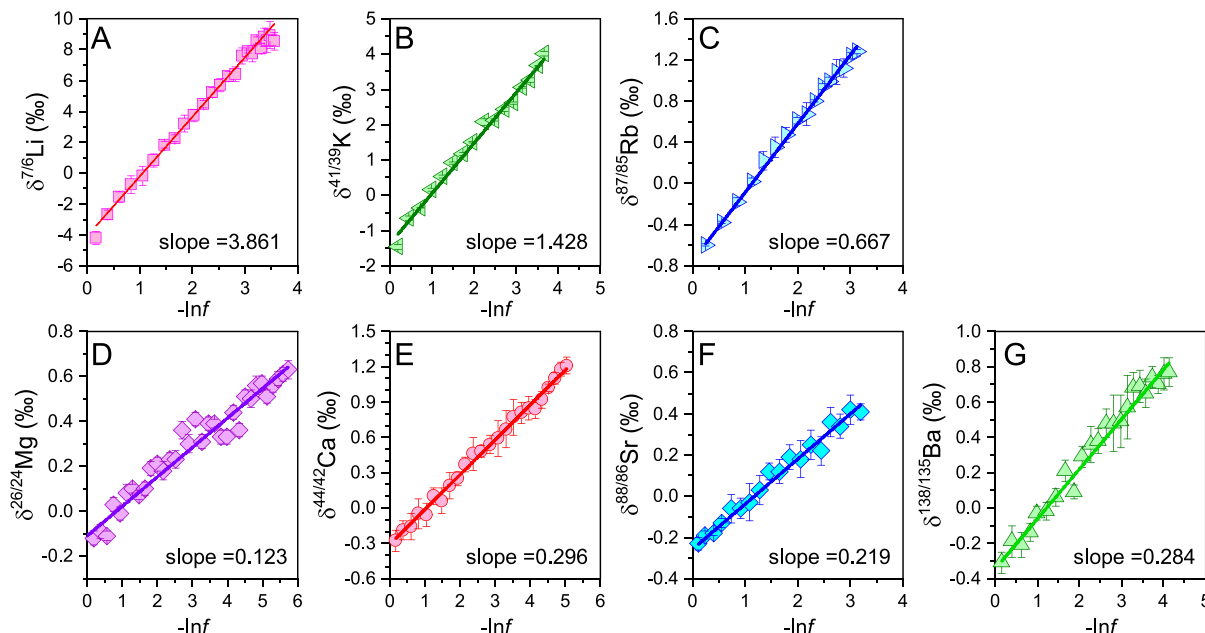


Fig. 4. Summary plot of the co-variation between δ and $-\ln f$ values of the solute in the tubes for diffusion experiments of Li (A), K (B), Rb (C), Mg (D), Ca (E), Sr (F), and Ba (G).

The mass-balanced average isotope composition of the solutes in the tubes and final cell, calculated using Eq. (2), are all close to 0 ‰ (within 0.2 ‰ for $\delta^7\text{Li}$, and within 0.06 ‰ for the rest of the isotope systems, Tables S3-1 to S3-7) for every experiment, supporting both the accuracy of mass spectrometry for each isotope system and the validity of the experiments.

In all experiments, the experimental data show excellent linearity in δ versus $-\ln f$ plots, which is also in accordance with Eq. (3) for the diffusion cell experimental concept. The slopes of the linear trends in each of the plots are obtained by linear regression using an Origin software (Fig. 4). Based on the slopes, the diffusion-driven isotope fractionation factor ($\alpha = 1 - \text{slope}/1000$) in aqueous solutions for the seven alkaline and alkaline-earth elements are obtained, which are: $\alpha_{7/6\text{Li}} = 0.996139 \pm 0.000140$, $\alpha_{41/39\text{K}} = 0.998572 \pm 0.000072$, $\alpha_{87/85\text{Rb}} = 0.999333 \pm 0.000020$, $\alpha_{26/24\text{Mg}} = 0.999877 \pm 0.000010$, $\alpha_{44/42\text{Ca}} = 0.999704 \pm 0.000010$, $\alpha_{88/86\text{Sr}} = 0.999781 \pm 0.000014$, $\alpha_{138/135\text{Ba}} = 0.999716 \pm 0.000018$ (Table 1). The uncertainties associated with the α factors are quantified as the uncertainties of slope regression by Origin software in Fig. 4. The fractionation factors and associated errors (2σ) can be expressed alternatively in $1000\ln\alpha$ (for ease of reading in ‰), which are: $1000\ln\alpha_{7/6\text{Li}} = -3.861 \pm 0.140$ ‰, $1000\ln\alpha_{41/39\text{K}} = -1.428 \pm 0.072$ ‰, $1000\ln\alpha_{87/85\text{Rb}} = -0.667 \pm 0.020$ ‰, $1000\ln\alpha_{26/24\text{Mg}} = -0.123 \pm 0.010$ ‰, $1000\ln\alpha_{44/42\text{Ca}} = -0.296 \pm 0.010$ ‰, $1000\ln\alpha_{88/86\text{Sr}} = -0.219 \pm 0.014$ ‰, $1000\ln\alpha_{138/135\text{Ba}} = -0.284 \pm 0.018$ ‰.

5.2. Comparison with previous studies

The isotope fractionation behavior of several alkaline and alkaline-earth elements during diffusion in aqueous solutions had been experimentally investigated using different methods and approaches. A comparison of the diffusion-driven isotope fractionation factors (α) obtained in this study and the previous studies are presented in Fig. 5. Specifically, isotope fractionation of Li during diffusion in aqueous solutions ($\alpha_{7/6\text{Li}}$) had been reported to be 0.99772 ± 0.00026 (Richter et al., 2006), 0.989 ± 0.003 (Fritz, 1992), and 0.9965 ± 0.002 (Kunze and Fuoss, 1962), our result (0.996139 ± 0.000140) is well within the reported $\alpha_{7/6\text{Li}}$ range. The experimentally determined $\alpha_{41/39\text{K}}$ (0.998572 ± 0.000072) in this study is higher than the $\alpha_{41/39\text{K}}$ (0.9979 ± 0.0002) reported by Bourg et al. (2010), which could be due to the difference in

temperature of diffusion experiments (25 °C in this study versus 75 °C in Bourg et al. (2010)), as diffusion-driven isotope fractionation in aqueous solutions has been suggested to be dependent on temperature (Eggenkamp and Coleman, 2009).

In terms of alkaline-earth elements (Fig. 5B), the diffusion-driven isotope fractionation factors of Ca ($\alpha_{44/42\text{Ca}} = 0.999704 \pm 0.000010$) and Ba ($\alpha_{138/135\text{Ba}} = 0.999716 \pm 0.000018$) obtained in this study are slightly lower than the corresponding values reported in previous studies (Bourg et al., 2010; van Zuilen et al., 2016). Additionally, Richter et al. (2006) reported an $\alpha_{26/24\text{Mg}}$ value of 1.00006 ± 0.00012 , which overlaps $\alpha = 1$ within uncertainty, meaning that isotopic fractionation between heavy and light Mg isotopes during diffusing in aqueous solutions was unresolvable in their study. For comparison, our experiments showed clear evidence of isotope fractionation during diffusion (Fig. 3D; Fig. 4D), with light Mg isotopes diffusing slightly faster than heavy Mg isotopes ($\alpha_{26/24\text{Mg}} = 0.999877 \pm 0.000010$), which is more consistent with the kinetic theory. Our results show that by combining the new experimental setup, higher data density, and improved analytical precision due to progresses in mass spectrometry in the past two decades, it is possible to distinguish subtle kinetic isotope fractionation effects of Mg cation diffusion in an aqueous solution.

To summarize, the α_{diff} factors obtained in this study generally match those experimentally determined by previous studies, with minor inconsistency that likely stemmed from differences in experimental settings. It should be highlighted that, because we applied the same method under the same condition to all the seven elements, the measured α_{diff} can provide an internally consistent basis for discussions on the intrinsic properties that govern diffusion-related isotope fractionation in aqueous solutions.

5.3. Mass dependence of isotope fractionation of cations during diffusion in aqueous solutions

Comparison of the kinetic isotope fractionation behaviors between elements requires the mass difference of isotopes to be normalized, which can be done using the following equation as proposed by Richter et al. (2006):

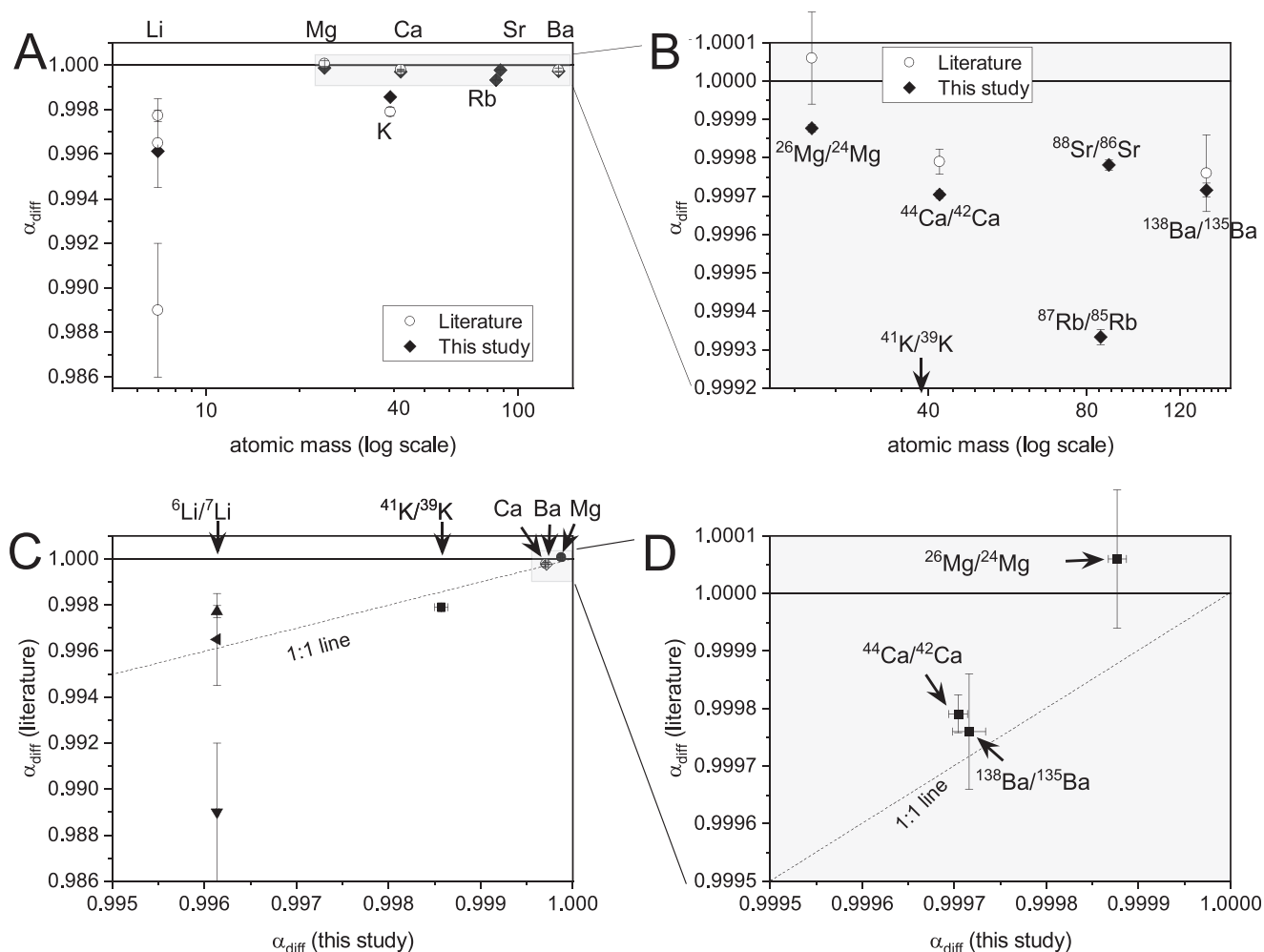


Fig. 5. Summary and comparison of experimentally determined isotope fractionation factors of alkaline and alkaline-earth elements during diffusion in aqueous solutions. Plot A summarizes all the available data with increasing atomic mass, plot B is the zoom-in of the upper-right corner of plot A to show details for Mg, Ca, Rb, Sr and Ba. Plot C compares the α_{diff} factors obtained in this study and those reported in literature; plot D is the zoom-in of the upper-right corner of plot A to show details for Ca, Mg, and Ba. Error bar denote 2σ uncertainty.

$$\alpha = \left(\frac{M_L}{M_H} \right)^\beta \quad (6)$$

where M_L and M_H are the masses of the light and heavy isotopes of interest, respectively, and β is the factor of mass dependence of isotopes during diffusion. In the case of maximum isotope fractionation effect such as diffusion of an ideal gas, β equals 0.5, an upper limit constrained by kinetic theory. In the case of no isotope fractionation effect, β equals 0, meaning that the diffusivity of ions in an aqueous solution is not affected by the mass of the isotopes at all. The β factor, varying between 0 and 0.5, therefore gauges the mass dependence of isotope diffusion for

different elements (Wanner and Hunkeler, 2019).

The β values for the seven alkaline and alkaline-earth elements are summarized in Table 1 and plotted in Fig. 3A. Alkaline elements are characterized by higher β values that are between 0.02 and 0.03, whereas the alkaline-earth elements have lower β values that are below 0.015. Notably, the two groups of elements define two separate trends on a plot of β versus $r_{\text{M-O}}$ (Fig. 6A), where $r_{\text{M-O}}$ is the average ion-water distance for the first hydration shell of ions (Ohtaki and Radnai, 1993). In each trend, β increases with $r_{\text{M-O}}$. Therefore, cation charge number and $r_{\text{M-O}}$ are the two primary factors that affect the β values of different elements in aqueous solutions.

Table 1

Summary of the slope data for the δ vs. $-\ln f$ plots (Fig. 4), and the corresponding α and β factors for the seven alkaline and alkaline-earth elements determined in this study.

Element	$r_{\text{M-O}}^*$ (Å)	Isotope ratio	Slope	2σ	α	2σ	β	2σ
Li	2.0	$^6\text{Li}/^7\text{Li}$	3.861	0.140	0.996139	0.000140	0.02510	0.00090
K	2.8	$^{41}\text{K}/^{39}\text{K}$	1.428	0.072	0.998572	0.000072	0.02857	0.00144
Rb	2.83	$^{87}\text{Rb}/^{85}\text{Rb}$	0.667	0.020	0.999333	0.000020	0.02869	0.00086
Mg	2.08	$^{26}\text{Mg}/^{24}\text{Mg}$	0.123	0.010	0.999877	0.000010	0.01154	0.00012
Ca	2.4	$^{44}\text{Ca}/^{42}\text{Ca}$	0.296	0.010	0.999704	0.000010	0.00636	0.00022
Sr	2.6	$^{88}\text{Sr}/^{86}\text{Sr}$	0.219	0.014	0.999781	0.000014	0.00953	0.00062
Ba	2.9	$^{138}\text{Ba}/^{135}\text{Ba}$	0.284	0.018	0.999716	0.000018	0.01292	0.00080

* data are from (Ohtaki and Radnai, 1993).

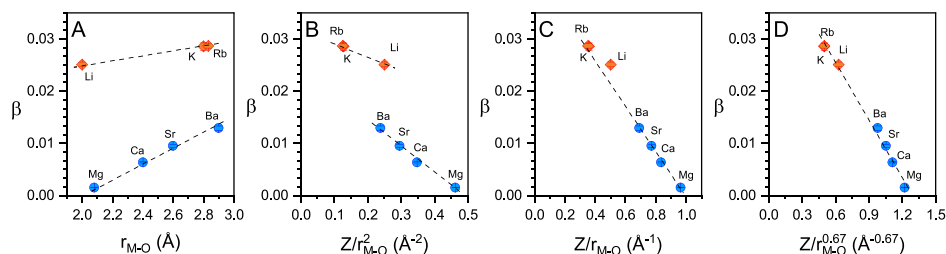


Fig. 6. A: Plot of β versus r_{M-O} for the seven elements in this study. B: Plot of β versus Z/r_{M-O}^2 for the seven alkaline and alkaline earth elements. C: Plot of β versus Z/r_{M-O} . D: Plot of β versus $Z/r_{M-O}^{0.67}$.

Alkaline-earth ions have twice the charge ($Z = +2$) compared to the charge of alkaline ions ($Z = +1$), thus ions of alkaline-earth elements have stronger interactions with the bipolar water molecules by forming the first and second hydration shells in aqueous solutions (Ohtaki and Radnai, 1993). At a molecular scale, there is a stronger friction between the hydrated aquo ions of the alkaline-earth elements and the surrounding water molecules through networks of hydrogen bonds (Baker, 2008). Such strong molecular friction results in the predominance of the hydrodynamic nature of the diffusing isotopes (i.e., the diffusion coefficient is almost uncorrelated with the mass of the isotope), thus β values are lower (closer to 0) for alkaline earth elements relative to alkaline elements. Given the same ionic charge, elements with longer r_{M-O} will have lower charge densities around the aquo ion, thus the ion-water interaction would be smaller. Subsequently, the aquo ions with longer r_{M-O} will have weaker molecular friction during diffusion in aqueous solutions and exhibit higher β values.

The relationships between β and cation charge number and r_{M-O} can be qualitatively rationalized by that the mass dependence of ion diffusion is controlled by the intensity of ion-water interaction. An intuitive quantification of such ion-water interaction is the surface charge density of the aquo ion around its first hydration shell (i.e., Z/r_{M-O}^2), however, on a plot of β versus Z/r_{M-O}^2 , the alkaline and alkaline-earth elements still plot along two different trends (Fig. 6B). In contrast, the two groups of elements plot along a linear trend more evidently on plots of β versus Z/r_{M-O} (Fig. 6C) and β versus $Z/r_{M-O}^{0.67}$ (Fig. 6D). It appears that Z/r_{M-O}^2 , the parameter for the hypothetical charge density around the sphere of the first hydration shell of ions, may not provide the best generalization of the ion-water interaction strength, as it does not account for the formation of the second hydration shell for high valence cations. Thus, the contribution of r_{M-O} needs to be reduced for better quantification of ion-water interaction between different element groups by using a formula of Z/r_{M-O}^n , and certain lower powder numbers (n) on r_{M-O} (i.e., Z/r_{M-O} in Fig. 6C and $Z/r_{M-O}^{0.67}$ in Fig. 6D) yield better linear trends for β factors of the investigated elements.

The observed trends of β factors may also be rationalized by considering the diffusion of aquo ion (cation with hydration shell) as a whole, that for a cation with more water molecules within its hydration shell, the relative mass difference caused by isotopic substitution is smaller, causing less significant kinetic isotopic effect during diffusion. However, as noted by Richter et al. (2006), such treatment alone would require an unrealistically large number of waters of hydration for Mg. Further, the kinetics of ion desolvation is dependent on the mass of the cation, causing isotope fractionation during exchange of water molecules in the first hydration shell of cations (Hofmann et al., 2012), and this isotopic effect is yet to be incorporated when considering the diffusion of aquo ion as a whole. Therefore, a simple kinetic model of idealized aquo ion diffusion is insufficient, although helpful for understanding the systematics of β factors for the cations. On the other hand, it has been reported that β factors of dissolved components correlate positively with the solvent-normalized diffusivity ($\log_{10}(D_i/D_{H_2O})$) (Watkins et al., 2011) and the water exchange frequency (k_{wex}) within the first hydration shell of aquo ions (Bourg et al., 2010). As noted in a review by Watkins et al. (2017), both $\log_{10}(D_i/D_{H_2O})$ and k_{wex} are

indexes of the strength of ion-water interaction. The results of our study (i.e., the correlation between β versus Z/r_{M-O}^n ; Fig. 6B–D) not only support such an idea but also further elucidate that the ion-water interaction strength originates from the surface charge density of the aquo ions, with surface charge and ion-water bond length being the primary controlling factor.

5.4. Applications and implications

The experimentally determined diffusion-driven kinetic isotope fractionation factors (Table 1) can be readily used for interpretations of isotope data of alkaline and alkaline-earth elements in supergene environments. For example, pore waters in seafloor sediment commonly exhibit downward changes in elemental and isotopic compositions of different cations as a result of early diagenesis, Table 1 provides updated α factors for Li, K, Mg, Ca, Ba isotopes and new α factors for Rb and Sr isotopes for numerical reaction-transport modelling studies of isotopic evolution of the diagenetic systems (e.g., Fantle et al., 2020; Higgins and Schrag, 2010; Santiago Ramos et al., 2018). Quantification of diffusion-driven isotope fractionation in aqueous solution is also critical for discussions of cation uptake mechanisms in organisms. For example, the determined $\alpha_{41/39K}$ (0.998572 ± 0.000072) for K isotopes suggests that a ~ 1.4 ‰ difference in $\delta^{41}K$ could be produced during *trans*-membrane transport of K just by chemical diffusion, and this magnitude is comparable to the K isotopic variability among plant tissues, animal tissues and extracellular fluids (Higgins et al., 2022; Li, 2017; Tacail et al., 2023). In light of this, enrichment of heavy K isotopes on the low-K side of the cellular membrane (i.e., opposite of diffusional isotope effect) could be safely identified as the consequence of active K-transporter activities on cell membranes; otherwise, biological effects (i.e., K channels) could not be directly distinguished from the effect of chemical diffusion.

In recent years, advances in mass spectrometry have expanded the use of stable isotopic tools in various applications (Teng et al., 2017), and novel isotopic tracers such as Rb stable isotopes and Sr stable isotopes are emerging (Wang et al., 2023; Zhang et al., 2021). According to isotope partition theories, the magnitude of the equilibrium isotope fractionation factor between two phases is inversely correlated with the square of the average mass of the isotopes (Bigeisen and Mayer, 1947; Schauble, 2004; Urey, 1947). Therefore, the magnitude of equilibrium isotope fractionation decreases rapidly for elements with increasing atomic mass, and so does the natural isotopic variability of the elements (Johnson et al., 2004; Teng et al., 2017). By contrast, our experimental results show that, during diffusion in aqueous solution, the kinetic isotope fractionation effect does not necessarily decrease with increasing atomic mass. On the contrary, β factors (as defined in Eq. (6)) increase with atomic mass number among the same group of alkaline or alkaline earth elements. This offsets the effect of relative mass difference that generally results in smaller isotope fractionation for heavier elements, and this offsetting effect is particularly prominent for alkaline earth elements, as the diffusion in aqueous solution causes can cause over 0.2 ‰ fractionation in $\delta^{138/135}Ba$, $\delta^{88/86}Sr$ and $\delta^{44/42}Ca$ values, compared with the ~ 0.1 ‰ fractionation in $\delta^{26/24}Mg$. Therefore, the

contribution of diffusion-driven kinetic isotope fractionation to natural isotopic variability might be significantly higher for heavier elements than lighter elements. Attention to diffusion is needed when studying stable isotope fractionation of Sr, Rb, and Ba in supergene environments where chemical disequilibrium take places.

6. Concluding remarks

- An efficient “diffusion-cell” method is developed to precisely determine diffusion-driven kinetic isotope fractionation factors of cations in aqueous solutions.
- Using the “diffusion-cell” method, diffusion-driven kinetic isotope fractionation factors (α) in aqueous solutions at 25 °C are experimentally determined for seven alkaline and alkaline earth elements. These factors are: $1000\ln\alpha_{7/6Li} = -3.861 \pm 0.140$ ‰, $1000\ln\alpha_{41/39K} = -1.428 \pm 0.072$ ‰, $1000\ln\alpha_{87/85Rb} = -0.667 \pm 0.020$ ‰, $1000\ln\alpha_{26/24Mg} = -0.123 \pm 0.010$ ‰, $1000\ln\alpha_{44/42Ca} = -0.296 \pm 0.010$ ‰, $1000\ln\alpha_{88/86Sr} = -0.219 \pm 0.014$ ‰, $1000\ln\alpha_{138/135Ba} = -0.284 \pm 0.018$ ‰
- The mass dependence of isotope fractionation during diffusion (β) varies between different elements and are primarily controlled by the the strength of cation-water interaction. Higher charge of the cation and shorter ion-water bond length for the aquo ion would cause less prominent kinetic isotope fractionation during diffusion in aqueous solutions, and vice versa.

Data availability

Data are available through Mendeley Data, at <https://doi.org/10.17632/2g2srd849f.1>.

CRediT authorship contribution statement

Weiqiang Li: Writing – review & editing, Writing – original draft, Visualization, Supervision, Methodology, Investigation, Funding acquisition, Formal analysis, Conceptualization. **Zhihan Ji:** Visualization, Investigation, Formal analysis. **Xianglong Luo:** Methodology, Investigation, Formal analysis. **Yuqi Li:** Methodology, Investigation.

Declaration of competing interest

The authors declare that they have no known competing financial interests or personal relationships that could have appeared to influence the work reported in this paper.

Acknowledgments

This study is supported financially by the National Natural Science Foundation of China (92358301, 41873004). This study is supported by the Fundamental Research Funds for the Central Universities (14380165, 14380126, 14380141 to WL). Prof. Xiaobin Cao is thanked for insightful discussions. This manuscript benefited greatly from constructive comments from three anonymous reviewers and editor-in-Chief Prof. Catalano.

Appendix A. Supplementary material

The **Supplementary Materials** contains (1) **Supplementary material S1**, which is a full mathematical proof of the key experimental concept of this study, (2) **Table S2**, which tabulates the detailed instrumental setting for analyses of Li, K, Rb, Mg, Ca, Sr, Ba isotopes using Nu 1700 Sapphire MC-ICP-MS, and (3) **Tables S3-1 to S3-7**, which are the detailed elemental and isotopic data table of all diffusion experiments reported in this study. Supplementary material to this article can be found online at <https://doi.org/10.1016/j.gca.2024.02.015>.

References

- Bakker, H.J., 2008. Structural dynamics of aqueous salt solutions. *Chem. Rev.* 108, 1456–1473.
- Bigeleisen, J., Mayer, M.G., 1947. Calculation of equilibrium constants for isotopic exchange reactions. *J. Chem. Phys.* 15, 261–267.
- Bourg, I.C., Richter, F.M., Christensen, J.N., Sposito, G., 2010. Isotopic mass dependence of metal cation diffusion coefficients in liquid water. *Geochimica Et Cosmochimica Acta* 74, 2249–2256.
- Bourg, I.C., Sposito, G., 2007. Molecular dynamics simulations of kinetic isotope fractionation during the diffusion of ionic species in liquid water. *Geochimica Et Cosmochimica Acta* 71, 5583–5589.
- Bourg, I.C., Sposito, G., 2008. Isotopic fractionation of noble gases by diffusion in liquid water: molecular dynamics simulations and hydrologic applications. *Geochimica Et Cosmochimica Acta* 72, 2237–2247.
- Cao, Z., Rao, X., Li, Y., Hong, Q., Wei, L., Yu, Y., Ehler, C., Liu, B., Siebert, C., Hathorne, E.C., Zhang, Z., Scholz, F., Kasten, S., Frank, M., 2023. Stable barium isotope fractionation in pore waters of estuarine sediments. *Geochem. Geophys. Geosyst.* 24, e2023GC010907.
- Christensen, J.N., Hofmann, A.E., DePaolo, D.J., 2019. Isotopic fractionation of potassium by diffusion in methanol. *ACS Omega* 4, 9497–9501.
- Eggenkamp, H.G.M., Coleman, M.L., 2009. The effect of aqueous diffusion on the fractionation of chlorine and bromine stable isotopes. *Geochimica Et Cosmochimica Acta* 73, 3539–3548.
- Fantle, M.S., Barnes, B.D., Lau, K.V., 2020. The role of diagenesis in shaping the geochemistry of the marine carbonate record. *Annu. Rev. Earth Planet. Sci.* 48, 549–583.
- Fritz, S.J., 1992. Measuring the ratio of aqueous diffusion coefficients between $6Li+Cl-$ and $7Li+Cl-$ by osmometry. *Geochimica Et Cosmochimica Acta* 56, 3781–3789.
- Higgins, J.A., Ramos, D.S., Gili, S., Spetea, C., Kanoski, S., Ha, D., McDonough, A.A., Youn, J.H., 2022. Stable potassium isotopes ($41K/39K$) track transcellular and paracellular potassium transport in biological systems. *Front. Physiol.* 13, 1016242.
- Higgins, J.A., Schrag, D.P., 2010. Constraining magnesium cycling in marine sediments using magnesium isotopes. *Geochimica Et Cosmochimica Acta* 74, 5039–5053.
- Hofmann, A.E., Bourg, I.C., DePaolo, D.J., 2012. Ion desolvation as a mechanism for kinetic isotope fractionation in aqueous systems. *Proc. Natl. Acad. Sci.* 109, 18689–18694.
- Jähne, B., Heinz, G., Dietrich, W., 1987. Measurement of the diffusion coefficients of sparingly soluble gases in water. *J. Geophys. Res.* 92, 10767–10776.
- Johnson, C.M., Beard, B.L., Albarède, F., 2004. *Geochemistry of Non-traditional Stable Isotopes*. Mineralogical Society of America; St. Louis, Washington, DC.
- Kunze, R.W., Fuoss, R.M., 1962. Conductance of the alkali halides. iii. The isotopic lithium chlorides. *J. Phys. Chem.* 66, 930–931.
- Li, W., 2017. Vital effects of K isotope fractionation in organisms: observations and a hypothesis. *Acta Geochimica* 36, 374–378.
- Liu, C., Li, W., 2023. Magnesium isotope fractionation between calcite and aqueous solutions under elevated temperatures of 98–170 °C. *Geochim. Cosmochim. Acta* 344, 160–177.
- Ohtaki, H., Radnai, T., 1993. Structure and dynamics of hydrated ions. *Chem. Rev.* 93, 1157–1204.
- O’Leary, M.H., 2002. Measurement of the isotope fractionation associated with diffusion of carbon dioxide in aqueous solution. *J. Phys. Chem.* 88, 823–825.
- Pinto de Magalhães, H., Brennwald, M.S., Kipfer, R., 2017. Diverging effects of isotopic fractionation upon molecular diffusion of noble gases in water: mechanistic insights through ab initio molecular dynamics simulations. *Environ. Sci. Processes Impacts* 19, 405–413.
- Richter, F.M., Mendybaev, R.A., Christensen, J.N., Hutcheon, I.D., Williams, R.W., Sturchio, N.C., Beloso, J.A.D., 2006. Kinetic isotopic fractionation during diffusion of ionic species in water. *Geochimica Et Cosmochimica Acta* 70, 277–289.
- Richter, F.M., Dauphas, N., Teng, F.-Z., 2009. Non-traditional fractionation of non-traditional isotopes: evaporation, chemical diffusion and Soret diffusion. *Chem. Geol.* 258, 92–103.
- Rodushkin, I., Stenberg, A., Andren, H., Malinovsky, D., Baxter, D.C., 2004. Isotopic fractionation during diffusion of transition metal ions in solution. *Anal. Chem.* 76, 2148–2151.
- Santiago Ramos, D.P., Morgan, L.E., Lloyd, N.S., Higgins, J.A., 2018. Reverse weathering in marine sediments and the geochemical cycle of potassium in seawater: insights from the K isotopic composition ($41K/39K$) of deep-sea pore-fluids. *Geochimica Et Cosmochimica Acta* 236, 99–120.
- Schauble, E.A., 2004. Applying stable isotope fractionation theory to new systems, *Geochemistry of Non-Traditional Stable Isotopes*. Mineralogical Soc America, Washington, pp. 65–111.
- Schulz, H.D., 2006. Quantification of early diagenesis: dissolved constituents in pore water and signals in the solid phase. In: Schulz, H.D., Zabel, M. (Eds.), *Marine Geochemistry*, second ed. Springer, Berlin Heidelberg New York, pp. 75–124.
- Stokes, R.H., 1950. An improved diaphragm-cell for diffusion studies, and some tests of the method. *J. Am. Chem. Soc.* 72, 763–767.
- Tacail, T., Lewis, J., Clauss, M., Coath, C.D., Evershed, R., Albalat, E., Elliott, T.E., Tütken, T., 2023. Diet, cellular and systemic homeostasis control the cycling of potassium stable isotopes in endothermic vertebrates. *Metallomics* 15.
- Teng, F.-Z., Dauphas, N., Watkins, J.M., 2017. Non-traditional stable isotopes: retrospective and prospective. *Rev. Mineral. Geochem.* 82, 1–26.
- Tyroller, L., Brennwald, M.S., Mächler, L., Livingstone, D.M., Kipfer, R., 2014. Fractionation of Ne and Ar isotopes by molecular diffusion in water. *Geochimica Et Cosmochimica Acta* 136, 60–66.

- Tyroller, L., Brennwald, M.S., Busemann, H., Maden, C., Baur, H., Kipfer, R., 2018. Negligible fractionation of Kr and Xe isotopes by molecular diffusion in water. *Earth Planet. Sci. Lett.* 492, 73–78.
- Urey, H.C., 1947. The thermodynamic properties of isotopic substances. *J. Chem. Soc.* 562–581.
- van Zuilen, K., Müller, T., Nägler, T.F., Dietzel, M., Küsters, T., 2016. Experimental determination of barium isotope fractionation during diffusion and adsorption processes at low temperatures. *Geochimica Et Cosmochimica Acta* 186, 226–241.
- Wang, J., Tarhan, L.G., Jacobson, A.D., Oehlert, A.M., Planavsky, N.J., 2023. The evolution of the marine carbonate factory. *Nature* 615, 265–269.
- Wanner, P., Hunkeler, D., 2015. Carbon and chlorine isotopologue fractionation of chlorinated hydrocarbons during diffusion in water and low permeability sediments. *Geochimica Et Cosmochimica Acta* 157, 198–212.
- Wanner, P., Hunkeler, D., 2019. Isotope fractionation due to aqueous phase diffusion – What do diffusion models and experiments tell? – A review. *Chemosphere* 219, 1032–1043.
- Watkins, J.M., DePaolo, D.J., Ryerson, F.J., Peterson, B.T., 2011. Influence of liquid structure on diffusive isotope separation in molten silicates and aqueous solutions. *Geochimica Et Cosmochimica Acta* 75, 3103–3118.
- Watkins, J.M., DePaolo, D.J. and Watson, E.B. (2017) Kinetic Fractionation of non-traditional stable isotopes by diffusion and crystal growth reactions. In: Teng, F.Z., Watkins, J., Dauphas, N. (Eds.), *Non-Traditional Stable Isotopes*, pp. 85–125.
- Zhang, Z., Ma, J., Wang, Z., Zhang, L., He, X., Zhu, G., Zeng, T., Wei, G., 2021. Rubidium isotope fractionation during chemical weathering of granite. *Geochimica Et Cosmochimica Acta* 313, 99–115.